Keith M. Beesley,[1] *B.Sc.; Savvas Damaskinos,*[1] *Ph.D; and A. E. (Ted) Dixon,*[1] *Ph.D.*

Fingerprint Imaging with a Confocal Scanning Laser Macroscope[2]

ABSTRACT: The scanning laser macroscope is a new scanning beam confocal imaging system that scans up to 7.5 cm × 7.5 cm in 5 seconds. One of its unique features is a telecentric f-theta lens that focuses the incoming beam from a low power laser to a 10 μm spot on the sample. The f-theta lens provides a linear scan, and has a flat focal plane. The macroscope is described in detail and its operation is discussed. Confocal reflected-light images of latent fingerprints were obtained on several different materials. Fluorescence images of Rhodamine-treated samples were also obtained. We also show a reflection image of a fingerprint recorded by scanning the finger in air. Other possible uses of the macroscope in forensics include time-resolved fluorescence, imaging of fluorescent gels used in DNA fingerprinting, IR fluorescence imaging of documents, detecting and recording fluorescence images of latent fingerprints excited with UV radiation, and entering file prints into the computer for storage.

KEYWORDS: forensic science, macroscope, fingerprints

Fingerprints are traditionally stored as ink prints on paper. This makes matching latent fingerprints with large files of stored prints difficult and time consuming. The development of the computer and scanning techniques allowed fingerprints to be stored digitally. This facilitates the retrieval of stored fingerprints so they can be compared rapidly with latent fingerprints in an investigation. Improving the development of latent prints on various materials has been the focus of investigation for a number of groups [1–4]; however, they are also interested in preserving, recording, and imaging the developed prints. In this work the macroscope developed at the University of Waterloo was used to image latent fingerprints on several different materials.

Latent fingerprints are often developed by cyanoacrylate fuming. One method is to vacuum deposit cyanoacrylate (crazy glue) onto the sample to form a protective coating over the print. In another method the deposition of cyanoacrylate takes place at room pressure in a heated environment. This method was used in preparing the samples used in this investigation. Fingerprints treated by either method can be imaged in reflected light.

Sometimes the fingerprint has poor reflective qualities, and in this case fingerprints are treated for fluorescence imaging. After cyanoacrylate fuming, the fluorescence treatment is performed by applying Rhodamine dissolved in methanol followed by the application of pure methanol to remove excess Rhodamine. This may be done either by spraying, or by immersing the sample in a Rhodamine-methanol solution and in methanol. The Rhodamine adheres to the cyanoacrylate covering the latent fingerprint, and is stripped away elsewhere by pure methanol. The Rhodamine will fluoresce when excited by 488 nm light.

Fingerprints on a variety of substrate materials have been investigated in this work. These include cyanoacrylate-treated latent fingerprints on a 20 cm × 40 cm clear plastic sheet and on a similar size piece of black plastic garbage bag material as well as untreated latent prints on glass and on a black polished surface (a silicon wafer). Images from Rhodamine-treated fingerprints were obtained in reflection and in fluorescence. Finally, a fingerprint was obtained by the direct imaging of a finger in air.

Description of the Confocal Scanning Laser Macroscope

The scanning laser macroscope is a new scanning beam confocal imaging system that forms a 512 × 512 image of a sample up to 7.5 cm by 7.5 cm in 5 seconds. The system uses a telecentric f-theta laser scan lens with a 10 μm spot size. The f-theta lens provides a linear scan, and has a flat focal plane. In addition, since the lens is telecentric, small changes in focus do not affect the magnification of the recorded image, as is the case with an ordinary microscope or camera. (NOTE: Although the present instrument uses a 512 × 512 pixel frame grabber to record images, it can be easily modified to acquire much more information from the specimen. For example, a $2\frac{1}{2}$ × 3 cm specimen, about the size of a thumbprint, can be digitized at 5 micron spacing as the focused spot travels across the specimen, resulting in a 5000 × 6000 pixel image. This has much higher resolution than the best video image, and similar resolution to a photographic emulsion.)

A ray diagram of the macroscope is shown in Fig. 1a. The incoming laser beam passes through a spatial filter and beam expander (SB) to produce a collimated beam 20 mm in diameter. The beam then passes through a beamsplitter (BS1) and is deflected by the first scanning mirror (SM1) through a unitary telescope (composed of two equal-focal-length lenses, L1 & L2) which brings the beam back on axis at the second scan mirror (SM2). SM2 is positioned at the entrance pupil of the laser scan lens (LSL) and reflects the 20 mm collimated beam into LSL. The laser scan lens focuses the beam onto the sample (S), light reflected from S is collected by LSL and travels back through the scan system to BS1. The beamsplitter deflects part of the signal into the detection arm where it is focused by a lens (CL1) onto a
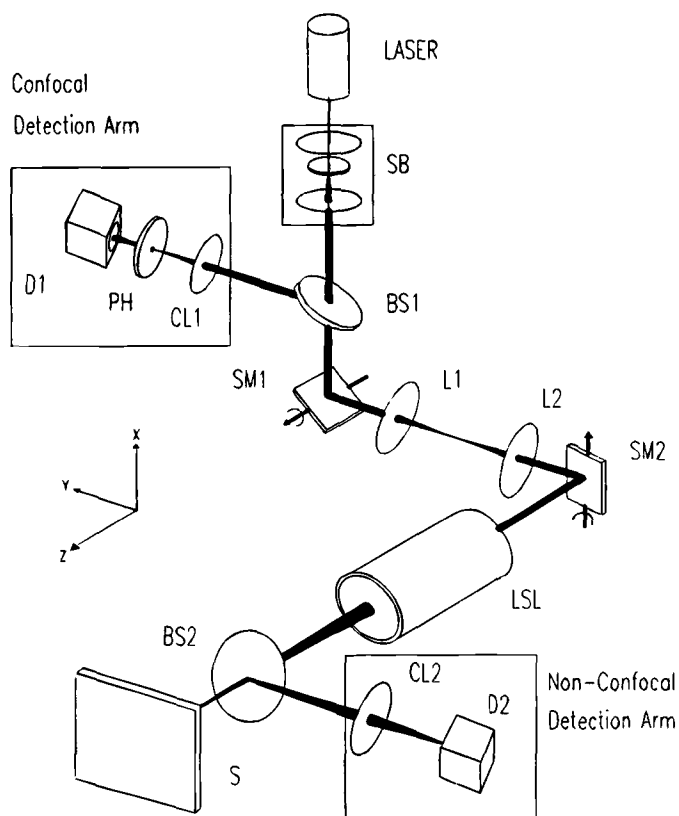
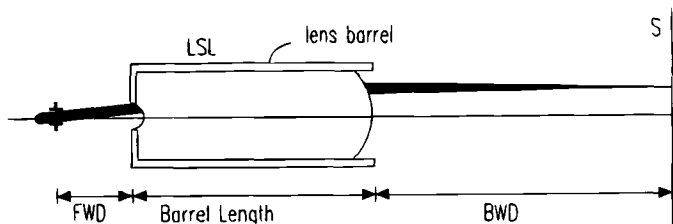FIG. 1a—*Ray diagram of the macroscope; scanning laser macroscope.*

FIG. 1b—*Ray diagram of the macroscope; telecentric laser scan lens.*

pinhole (PH). Because the pinhole is confocal with the illuminated spot on the sample, light from above or below the focal point will not pass through the pinhole, and is not detected by detector D1. Thus confocal images contain in-focus information only, and the instrument is capable of performing optical tomography. In addition a separate non-confocal detector has been implemented on the macroscope. This was accomplished by placing a beamsplitter (BS2) in the path between LSL and the sample as shown in Fig. 1a. Light reflected from the sample is now deflected by BS2 into a collector lens (CL2) that focuses the beam onto detector (D2). Images are detected by scanning the focused spot across the sample in a raster scan.

If the macroscope is to be used in fluorescence, a multiwavelength ArKr laser can be used instead of the HeNe laser. In this case the 488 nm laser line is selected with a bandpass filter. The current setup shown in Fig. 1a can image in fluorescence in both confocal and non-confocal modes. For confocal fluorescence a dichroic beamsplitter that transmits the laser light (~80% transmission) and reflects the fluorescent light (~90% reflection) is placed

at BS1. Fluorescent light emitted from the sample is collected by LSL and travels back to the dichroic beamsplitter at BS1 where it is directed into the detection arm of the macroscope. A long-pass filter passes the fluorescent light while further reducing the reflected laser beam and other extraneous light. Fluorescence from the focused spot on the sample passes through PH and is measured by the detector. For samples with weak fluorescent emission the macroscope is operated in the non-confocal mode that uses detector D2 since the small numerical aperture (NA) of the LSL makes it difficult to detect low-level fluorescence emission at the confocal detector. In this case fluorescence emitted from the sample is deflected by a large dichroic beamsplitter at BS2 into a long-pass filter that passes the emitted fluorescence and blocks the reflected laser beam. The fluorescence is then focused by a collector lens onto detector D2 where it is measured. Since the macroscope focuses the laser beam to a spot of 5 microns radius, 0.5 mW of laser power results in a power density of 200 W/cm² at the focused spot. This should be compared with the conventional technique of expanding the beam of a high power laser to illuminate a fingerprint for fluorescence imaging. A 10 W laser expanded to fill a 7.5 cm diameter circle results in a power density of only 0.23 W/cm² at the sample position. Thus the macroscope is potentially a much smaller and less expensive instrument for detecting latent prints using fluorescence.

A telecentric laser scan lens is shown in Fig. 1b. The telecentric property of the lens causes the cone of light incident on the sample to be perpendicular to the sample at any position, resulting in a uniform intensity throughout the scan in reflection. The f-theta property of the lens means the position of the focal point on the sample changes linearly with the angle of the beam entering the lens. A scan with uniform velocity is then achieved by having the mirrors scan at constant angular speed and a constant sampling rate is used to record the data.

A photograph of the actual experimental setup is shown in Fig. 2. The laser beam travels from the ArKr laser (top right), along the back of the optical table to reach the first scanning mirror (top left) and is deflected toward the second scanning mirror and the laser scan lens (bottom left). A clear plastic sheet containing fingerprint specimens is shown in front of the laser scan lens.

Results

The following fingerprint images illustrate some of the capabilities of the macroscope. These images were obtained by scanning
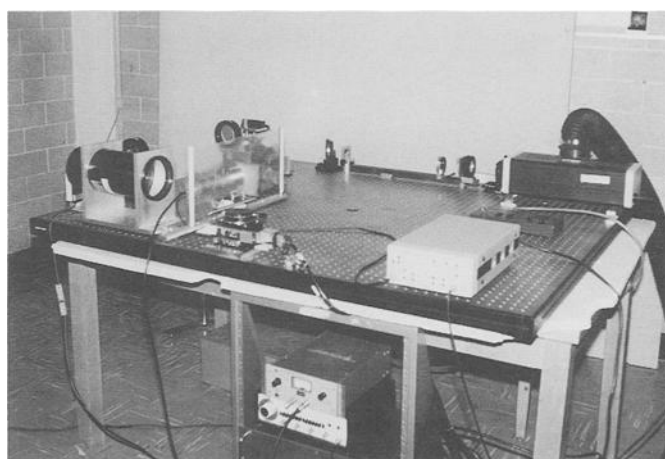

FIG. 2—*The experimental setup.*

3 different ranges. The first range covered a 6 cm × 6 cm area (magnification 1×), which allows images containing several fingerprints to be recorded. A higher resolution image of an entire single fingerprint is obtained by scanning a 3 cm × 3 cm area (magnification 2×). The pores on the ridges of the fingerprint become more evident in a smaller scan of 1.5 cm × 1.5 cm (magnification 4×) which images only part of a fingerprint.

Figure 3 shows a confocal reflected-light image of a 6 cm × 6 cm area of cyanoacrylate treated fingerprints on clear plastic. Three fingerprints corresponding to the index, middle and ring fingers are clearly seen. The contrast is provided by the difference in reflection between the fingerprint itself and the clear plastic. It appears that a substantial amount of incident light (at 633 nm) is scattered by the fingerprint which results in reduced light collection by the laser scan lens and a smaller signal measured at the confocal detector. The cyanoacrylate-treated clear plastic sample includes several folds as well as a number of minor defects that are visible to the naked eye. A major fold running vertically is clearly seen near the middle of the image. The dark line at the fold is due to the low numerical aperture (0.055) of the laser scan lens which means light reflected away from the normal to the plastic sheet is not collected by the laser scan lens. Some other minor defects in the plastic sheet are also visible in the image.

In Fig. 4 higher magnification confocal images of the fingerprint on the left in Fig. 3 are shown in reflection. The top image is a confocal slice of a 3 cm × 3 cm area of the fingerprint. A single fingerprint is now imaged and the increased resolution provides a more detailed observation of the fingerprint. The vertical fold is still present as well as a portion of the central fingerprint seen in Fig. 3. The bottom image in Fig. 4 shows an even higher magnification of the same fingerprint. The area scanned is now reduced to 1.5 cm × 1.5 cm. This results in even greater detail, and pores in the ridges of the fingerprint are now becoming visible.

Figure 5 shows confocal image slices in reflected light of a

FIG. 4a—*Cyanoacrylate-treated fingerprint on clear plastic; entire fingerprint. Field of view is 3 cm × 3 cm.*

FIG. 4b—*Magnified image of part of the above fingerprint. Field of view is 1.5 cm × 1.5 cm. 5 mW HeNe laser with O.D. 3.0 ND filter.*

FIG. 3—*Cyanoacrylate-treated fingerprints on clear plastic. Field of view is 6 cm × 6 cm. The intensity of the incoming beam from the 5 mW HeNe laser has been reduced by a factor of 1000 using an O.D. 3.0 neutral density filter.*

fingerprint on black garbage bag material. The image of a complete fingerprint is shown in Fig. 5a. The contrast here is again due to the difference in reflection between the fingerprint and the plastic. However, unlike the clear plastic sample where background reflection is relatively uniform (see Fig. 4) a black garbage bag may become readily wrinkled and damaged. The numerous folds created in the plastic behave as scattering centers that can degrade the
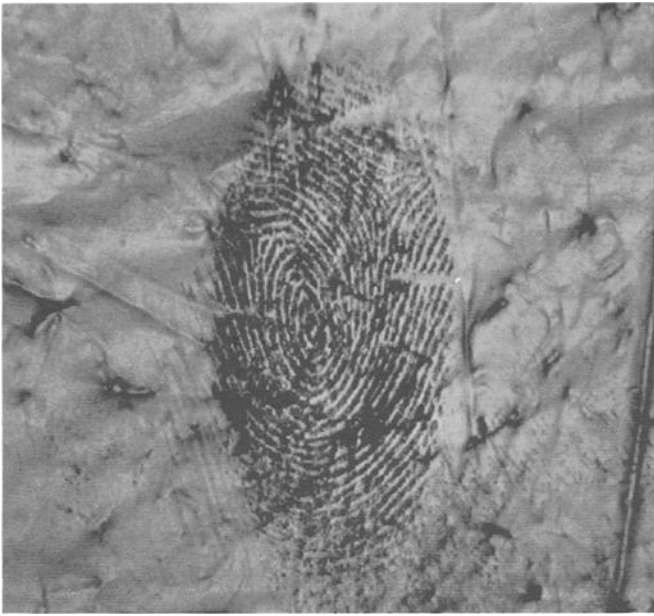
FIG. 5a—Cyanoacrylate-treated fingerprint on black garbage bag material; entire fingerprint. Field of view is 3 cm × 3 cm.

FIG. 6a—Untreated fingerprint on the polished surface of a silicon wafer; entire fingerprint. Field of view is 3 cm × 3 cm.

FIG. 5b—Magnified image of part of the above fingerprint. Field of view is 1.5 cm × 1.5 cm. 5 mW HeNe laser with O.D. 3.0 ND filter.

FIG. 6b—Magnified image of part of the fingerprint. Field of view is 1.5 cm × 1.5 cm. 5 mW HeNe laser with O.D. 3.0 ND filter.

image of a fingerprint. Despite this the fingerprint image appears relatively clean and considerable detail can be seen. The bottom image is a higher magnification image of the same fingerprint. The segment of the fingerprint imaged shows good contrast. The pores in the ridges of the fingerprint are now visible while the folds in the garbage bag do not appear to dominate or degrade the image to any significant degree.

Figure 6 shows confocal images in reflection of an untreated fingerprint on the surface of a polished silicon wafer. The top image shows an almost complete thumbprint while the bottom image shows a magnified image of a large segment of the same fingerprint. Scattering of the incoming light by the fingerprint remains the main contrast mechanism in these images. The pores

in the ridges of the fingerprint are clearly visible in the higher magnification image. The intensity variation seen in the top image is in part due to the wafer not being perpendicular to the incoming beam so that the bottom of the image is out-of-focus in the confocal image slice, and also due to a non-uniform wafer surface. The signal intensity appears to be relatively uniform in the higher magnification image. Figure 7 shows images of an untreated fingerprint on a glass substrate. The top image shows a complete thumbprint while the bottom image shows a magnified image of a segment of the same fingerprint.

Figure 8 shows nonconfocal images in reflection and in fluorescence of a Rhodamine-treated fingerprint on clear plastic. In Fig. 8a the reflected-light image is obtained by focusing the laser beam onto the sample surface from the fingerprint side. In Fig. 8b the
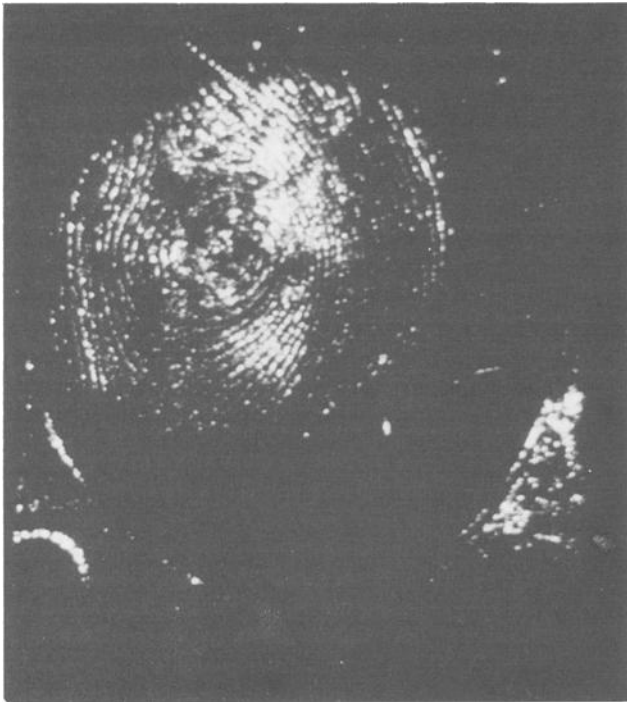
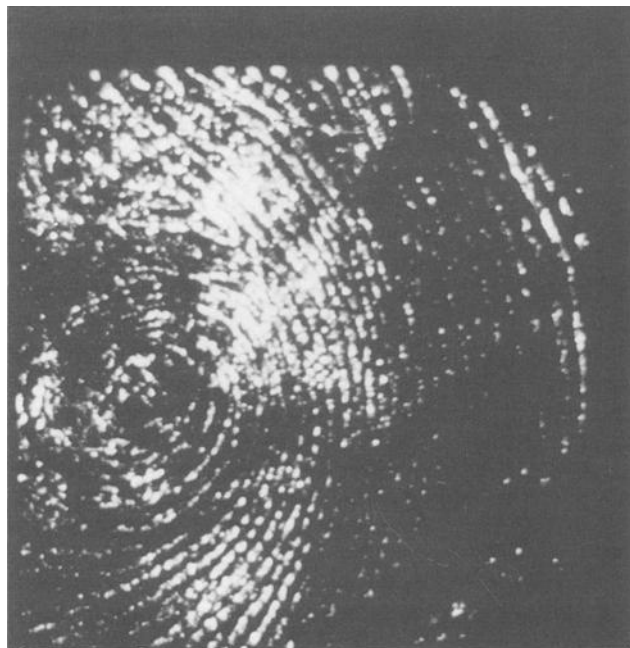FIG. 7a—Untreated fingerprint on glass; (a) entire fingerprint. Field of view is 3 cm × 3 cm.

FIG. 7b—Magnified image of part of the fingerprint. Field of view is 1.5 cm × 1.5 cm. 5 mW HeNe laser with O.D. 2.0 ND filter.

reflected-light image of the same fingerprint is obtained after rotating the sample by 180° and focusing the laser beam onto the fingerprint through the clear plastic. Note that the two images are mirror images of each other. Data extracted from these images show: (a) that the reflectivity of the clear plastic surface is always larger than that of the fingerprint, and remains relatively constant independent of the direction from which the laser beam is focused and (b) that the reflectivity of the fingerprint through the clear

plastic is 1.5 to 2 times the reflectivity measured from the same side as the fingerprint. The difference in reflectivity (reflectivity of clear plastic surface—reflectivity of fingerprint) has resulted in a higher contrast image when obtained from the same side as the fingerprint. This can be explained in terms of reduced light scattering at the fingerprint. The print-plastic interface can be considered as a flatter surface than the top surface texture of the fingerprint. This smoother interface will increase specular reflection resulting in the difference in reflectivity between the top and bottom surfaces of the fingerprint.

Figures 8c and 8d show nonconfocal fluorescence images of the same fingerprint obtained from the print side and from the opposite side through the clear plastic. The fluorescence images have an intensity distribution that is opposite to that of the reflected-light images, giving a bright signal from the ridges. This makes the pores on the ridges more evident than in the reflection images. Data extracted from these two images show: (a) that background fluorescence of the clear plastic surface is about the same independent of the direction through which the laser beam is focused and (b) that fluorescence intensity from the fingerprint through the clear plastic is only slightly less than the fluorescence measured from the same side as the fingerprint. A smear is evident in both the fluorescence and reflected light images, which may be the result of the print being partially smudged since the smear fluoresces.

Finally Fig. 9 shows reflected-light images of a fingerprint recorded by directly scanning a finger in air. The top image shows the entire fingerprint while the bottom image is a view of a smaller region of the same fingerprint. The 50 μm diameter pinhole in front of the detector was replaced with a 1 mm diameter iris diaphragm for this measurement. This makes the images substantially non-confocal and increases the depth of field to several millimeters thus allowing a substantial area of the finger to be seen in a single frame. The direct imaging of a finger in air was accomplished by building a mount that holds the finger steady for 5 seconds, which is the acquisition time for a 512 × 512 image by the macroscope.

Discussion

A new scanning beam system that is confocal and can image large specimens up to 7.5 cm × 7.5 cm has been briefly described. This unique system uses a telecentric f-theta laser scan lens as the imaging objective lens, is confocal and can be used both for reflection and fluorescence imaging. For weak fluorescence specimens a second non-confocal detector has been implemented as shown in Fig. 1a. The collection NA in fluorescence using the second detector can be as high as 0.5 compared to a 0.055 collection NA through the laser scan lens for confocal imaging. In addition the small number of optical surfaces required when the second detector is used ensures maximum photon collection efficiency.

In this work, the macroscope has been used to image fingerprints on a variety of substrate materials. The images presented in the previous section clearly show some of the advantages of the system. High contrast, low magnification images of latent fingerprints have been obtained in reflection as well as higher magnification images of single fingerprints in both reflection and fluorescence. Sharp images of the cyanoacrylate-treated fingerprints have been obtained on clear plastic. The folds and wrinkles in the plastic do not appear to have a significant detrimental effect on the fingerprint image. The pores on the ridges of the finger are clearly visible in the higher magnification images. A conventional microscope reveals that dark plastic garbage bags are colored by small dark

FIG. 8a—Rhodamine-treated fingerprint on clear plastic. Field of view is 3 cm × 3 cm; (a) reflection image. The laser beam is focused onto the sample surface from the fingerprint side.

FIG. 8b—Reflection image. The laser beam is focused onto the sample surface through the clear plastic.

FIG. 8c—Fluorescence image. The laser beam is focused onto the sample surface from the fingerprint side.

FIG. 8d—Fluorescence image. The laser beam is focused onto the sample surface through the clear plastic. 60 mW ArKr laser plus 10 nm narrow bandpass filter centered at 488 nm. Measured power at 488 nm incident on the sample = 0.5 mW. An O.D. 4.0 ND filter was used in front of the detector for the reflected-light images only.
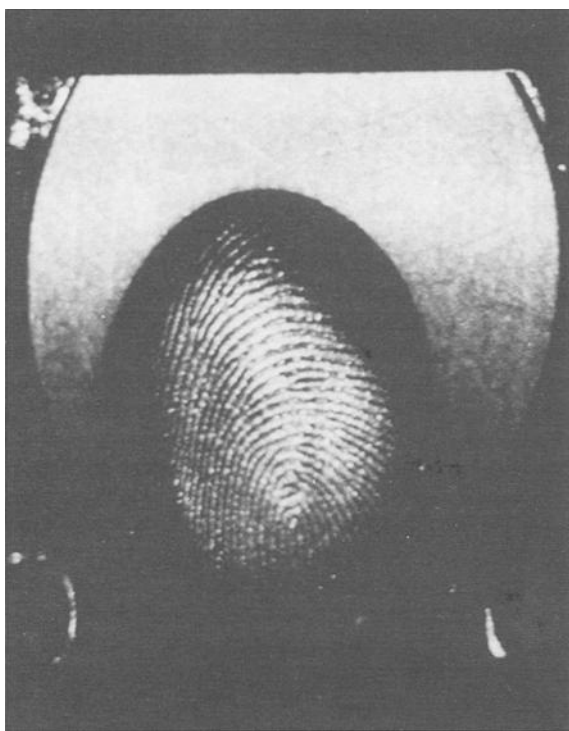
FIG. 9a—*Finger scanned directly in air;* (a) *entire finger. Field of view of 3 cm × 3 cm.*

FIG. 9b—*Magnified image of part of the finger. Field of view of 1.5 cm × 1.5 cm. 5 mW HeNe laser.*

particles in the plastic. Fingerprints on the garbage bag viewed with the macroscope did not show these particles, instead high contrast images were obtained in reflection. Sometimes only small segments of damaged fingerprints can produce good images. High resolution images of these partial fingerprints can still lead to fingerprint identification.

Untreated prints on a glass substrate and on a silicon wafer also produced good images. When a series of fingerprints must be obtained from the same surface, for example when fingerprints are taken at a police station, it is an advantage if the fingerprints do not require any treatment, so that the surface can be easily wiped clean before the next set of prints are taken.

Preliminary results show that Rhodamine-treated fingerprints on clear plastic can be imaged both in reflection and fluorescence. These nonconfocal results show that fingerprints can be examined both from the side that includes the fingerprints as well through the clear plastic. In reflection, the image through the clear plastic is of lower contrast than the direct image. In fluorescence there appears to be no significant difference between the two images. Because the signal that forms the images in fluorescence originates from the residue of the fingerprint the pores on the ridges can be more visible in this mode than in reflection. Also fluorescence is an additional important method of fingerprint examination for surfaces that have poor reflective properties. Fluorescence may allow examination of fingerprints that cannot otherwise be examined (they may be on a rough surface, poorly reflecting surface, etc.), which makes this method of imaging useful.

Direct scanning of a finger in air has also been attempted with the macroscope and reasonably good images have been obtained. This method of imaging has the advantage of being relatively fast (it is currently 5 seconds per scan, but this could be shortened to 1 second per scan) and in addition it eliminates the problem of previous latent fingerprints if the finger is held against a glass plate. Such a technique can be used in police stations for taking fingerprints directly at the time of booking. It is fast, requires no additional material and the result is a digitized high contrast fingerprint image that is stored in the computer and takes no physical storage room.

Other possible uses of the macroscope are as follows: a) Existing fingerprints on file cards can be digitized for storage into a computer that will allow faster access and comparison during criminal investigations as well as providing a better filing system. b) The macroscope is a relatively simple system that uses a low power laser (5–60 mW) with a minimum of moving mechanical components (two scanning mirrors) that can be packaged as a portable system for acquiring fingerprint evidence during criminal investigations. c) Another potential use of the macroscope is for time-resolved imaging [5] of fingerprints on strongly luminescent materials. The development of new fluorophores [6] with slow fluorescence decay times (on the order of 1 ms) that can be preferentially attached to the latent fingerprint on a substrate can be used to separate the fingerprint fluorescence signal from the substrate fluorescence signal that decays very fast (on the order of 1 nanosecond). This can be accomplished by chopping the incoming laser beam and gating the detector to show only the fluorescence from the fingerprint. The macroscope can be modified to perform such an experiment. The high collection NA of the non-confocal detector ensures a large signal-to-noise ratio when an incident beam of low intensity is used, thus preventing fluorophore saturation or bleaching. d) In addition there is some interest in the development of other fluorophores that are usable in the Ultraviolet region (UV) and in the Infrared Region (IR) of the spectrum. The macroscope can be readily adapted for use in the near-UV region (>0.4 μm)

and in the near-IR region (up to 2.0 μm). e) Another possible application is for reading fluorescent gels in DNA fingerprinting. The fingerprint images shown in this work are photographs obtained directly from the computer screen. This method of presentation produced the highest contrast images of all of the methods available to us.

Acknowledgments

References

[1] Dalrymple, B. E., Duff, J. M., and Menzel, E. R, "Inherent Fingerprint Luminescence-Detection by Laser," *Journal of Forensic Sciences*, Vol. 22, No. 1, 1977, pp. 106–115.

[2] Herod, D. W. and Menzel, E. R, "Spatially Resolved Fluorescence Spectroscopy: Application to Latent Fingerprint Development," *Journal of Forensic Sciences*, Vol. 28, No. 3, July 1983, pp. 615–622.

[3] Menzel, E. R., Burt, A. J., Sinor, W. T., Tubach-Ley, W. B., and Jordan, J. K., "Laser Detection of Latent Fingerprints: Treatment with Glue Containing Cyanoacrylate Ester," *Journal of Forensic Sciences*, Vol. 28, No. 2, April 1983, pp. 307–317.

[4] Saunders, J. C., "Macroscopic Examination of Overlapping Latent Prints on Non-Porous Items," *Journal of Forensic Identification.*, Vol. 43, February 1993, pp. 138–143.

[5] Murdock, R. H. and Menzel, E. R., "A Computer Interfaced Time-Resolved Luminescence Imaging System," *Journal of Forensic Sciences*, Vol. 38, No. 3, May 1993, pp. 521–529.

[6] Mekkaoui, A. I. and Menzel, E. R., *Journal of Forensic Sciences*, Vol. 38, No. 3, May 1993, pp. 506–520.

Address requests for reprints or additional information to:
A. E. Dixon, Ph.D.
Dept. of Physics
University of Waterloo
Waterloo, Ontario N2L 3G1
Canada